Experimental definition of valence-shell and cumulative-shell Compton profiles from 25-keV electron-impact studies on N_2, Ne, and Ar†

T. C. Wong,* J. S. Lee, H. F. Wellenstein,‡ and R. A. Bonham
Department of Chemistry, Indiana University, Bloomington, Indiana 47401
(Received 27 February 1975)

The maximum and high-energy loss side of the Bethe ridge, obtained from high-energy electron-impact spectroscopic observations with 25-keV electrons, has been interpreted in terms of an effective Compton profile, $J_{\text{eff}}(q, K)$ defined in terms of the absolute generalized oscillator strength (GOS) $f(K, E)$ as $J_{\text{eff}}(q, K) = (2K^3/E) f(K, E)$, where q is $(E-K^2)/2K$ with K the momentum transfer and E the energy loss. It is well known that for He and H_2 this effective profile for constant q approaches the x-ray Compton profile in the limit of large K for fixed but large incident-electron energy. We report here the discovery of plateaus in the envleope of $J_{\text{eff}}(q, K)$ for constant q with increasing K, in addition to the x-ray profile limit, for target systems containing more than one shell. In the cases of N_2 and Ne, an additional plateau is observed which is associated with the outer-shell electrons because the maximum of the Bethe ridge has not yet reached the energy-loss region of core or K-shell excitations. This additional plateau makes it possible to define an effective outer-shell Compton profile. In the case of argon, two plateau regions are observed before the Bethe ridge reaches the K-shell contributions and effective profiles are defined for the M and M-plus-L shells. Comparisons with theory suggest that the cumulative-shell Compton profiles agree with direct theoretical computations utilizing the x-ray formula but including only contributions from the shell(s) in question at the 5% accuracy level. On the other hand, computations of the GOS using explicit final-state ion wave functions agree with our experiments at the (1–2)% level.

I. INTRODUCTION

In 1923, Compton[1] observed a broad spectral line attributed to large-angle inelastically scattered x rays, and later DuMond[2] derived a Doppler-broadening theory which pointed out that this line, referred to as a Compton profile, should be ideal for the study of the momentum distributions of target electrons in atoms and molecules. In 1938, the experiments of Hughes and Mann[3] showed that inelastic electron scattering displayed the same characteristic Compton peak. However it has not been until recently, with the rapid development of new experimental techniques, that sufficiently accurate experimental Compton scattering results were obtained to make meaningful comparisons with theory possible.

The most commonly used of these modern techniques are x-ray,[4] γ-ray,[5] and high-energy electron[6] scattering. Interesting applications of Compton profile studies include topics such as the effects of electron correlation,[7] chemical bonding,[8] localized orbitals,[9] and molecular vibrations[10] on Compton peaks. These have been investigated both experimentally and theoretically. Most of these effects have been shown to be significant only for the valence or conduction electrons. Heretofore, however, all x-ray and γ-ray experiments have been used to obtain only the total Compton profile. Reported "experimental" valence profiles from these studies were actually deduced by subtracting from the total profile the calculated Compton profile for the inner-shell electrons (in most cases, 1s electrons).

While it was generally believed that the core Compton profile is reasonably well understood, a recent theoretical study by Smith and Whangbo[11] showed that there were significant differences between the momentum-space properties of localized and canonical orbitals for core electrons in molecules. Therefore, the "experimental" valence profile will also be affected by this ambiguity in defining the core electron contribution to the Compton profile, at least in the molecular case. If the core electrons are other than 1s electrons, the uncertainty can be so large that poor agreement results between experiment and rigorous calculations, as exemplified by the experimental studies of the valence-band Compton profiles of[12] Fe and Ge.[13] Therefore a direct measurement of the valence Compton profile should be of interest, and in some cases the only way to infer valence-electron momentum-space properties.

There have been several theoretical calculations for valence Compton profiles[14] in which the contribution from various orbitals are separately calculated. Recently, the development of the angular correlation $(e, 2e)$ technique[15] which measures

both the scattered and ejected electrons in coincidence, offers a new and attractive method for determining the electron momentum distribution (EMD) for separate one-electron orbitals provided that orbital energy differences are sufficiently larger than the energy resolution of the experiment.

In this paper, we report the discovery of a possible way for directly measuring the valence Compton profiles for atoms and molecules. The idea behind the experiments reported here stems from the nature of the structure of experimental generalized oscillator strength (GOS) curves, the totality of which suffice to define a Bethe surface.[16] A study of the Bethe surface which is proportional to the cross-section differential with respect to the solid angle of the scattered electron and the energy loss as a function of scattering angle and energy loss for[17] N_2 at small scattering angles suggests a natural separation of the spectrum into two parts. The spectrum, as experimentally determined for N_2, is shown in Fig. 1. The first part from 9 to 400 eV in energy loss is presumably associated with excitation of valence-shell electrons, while the spectrum beyond 400 eV, with the exception of an apparently small underlying overlap with the valence shell, is associated with core excitations. In fact, making allowance for the underlying valence overlap in the core region as outlined in Sec. IV, we estimate from our experimental data that the ratio of the area of the GOS in the valence region to the area of the GOS of the core region to be $\frac{10}{4}$ to within ±0.5 electrons.

As the scattering angle or momentum transfer increases from zero angle, the maximum continuum contribution, initially centered at 15–20 eV in energy loss, moves to higher-energy loss, forming a definite peak. It is clear from Fig. 1 that this continuum maximum as a function of momentum transfer K forms a dominant ridge, referred to as the Bethe ridge, which takes on the characteristic shape usually associated with a Compton profile well before the ridge passes through the K shell or core spectral region beginning at 400 eV. The obvious question is whether the Bethe ridge, devoid of core electron contributions, can indeed be meaningfully analyzed in terms of a Compton profile. Hence the main purpose of this study will be to investigate in detail the regions of the maximum and the high-energy loss side of the Bethe ridge, before it passes through the energy loss for excitation and ionization of the next innermost shell(s), in terms of a Compton profile. Effective Compton profiles for the valence shell of N_2, the L shell of Ne, the M shell of Ar, and the M-plus-L shells of Ar will be investigated in this endeavor. The total Compton profile in N_2 will also be measured in order to extract an estimate of the core electron Compton profile. Total profile determinations for Ne and Ar are beyond the angular range capability of our present experimental equipment.

II. THEORY

An approximate theoretical analysis of the present experiment and the extraction of the Compton profile from the GOS have been given in detail elsewhere.[18,6] The exact first Born expression for the total inelastic scattering cross section in-

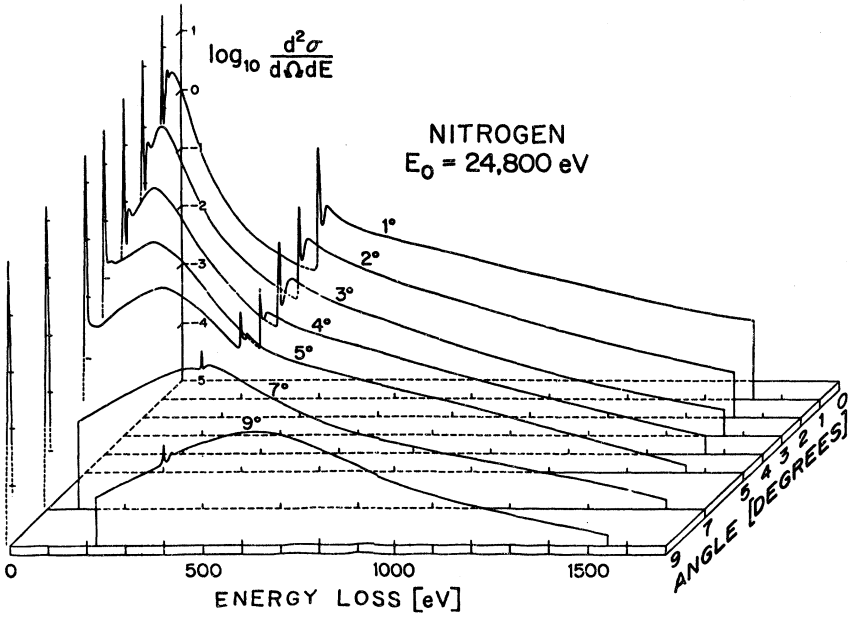

FIG. 1. Plot of the relative cross-section differential with respect to scattered electron solid angle and energy loss $d^2\sigma/d\Omega dE$ as a function of scattering angle θ and energy loss E. Note that the surface displayed by this plot is qualitatively similar to a Bethe surface.

cluding exchange effects was developed in an expansion in powers of $\hbar$ in Ref. 18, where the zeroth-order term was found to correspond to the quantum-mechanical binary encounter model. In this model each incident electron is scattered by at most two target electrons, and conservation of energy and linear momentum are satisfied for the initial collision only. The correction to the binary encounter model proportional to $\hbar$ was investigated and was found to be small for sufficiently large momentum transfer. However this does not rule out the possibility of a large correction due to slow convergence of the expansion. The theory was simplified by an approximate factorization which separated the interference and exchange correction from the direct scattering.

The electron Compton profile can be extracted from a cross section of the Bethe ridge taken at constant momentum transfer, where the position at the maximum is approximately given as $E = K^2 - E^2/4c^2$ by use of relativistic kinematics, where E is the energy loss, K is the momentum transfer, and c is the velocity of light, and all quantities here and in the following are expressed in Rydberg atomic units. The result for the cross-section differential with respect to the solid angle of the scattered electron and its energy loss to the target $d^2\sigma/d\Omega\, dE$, often called the second-order differential cross section, is given approximately in terms of the effective Compton profile in the binary encounter theory as

$$\frac{d^2\sigma}{dE\,d\Omega} = \frac{2k(E)[1 - E(1-\beta^2)^{1/2}/2c^2]\,F_{ex}^R}{k(1-\beta^2)K(K^2 - E^2/4c^2)^2}\, J_{\rm eff}(q,K), \tag{1}$$

where k and $k(E)$ are the incident and scattered momenta, respectively, F_{ex}^R is the correction for exchange scattering given in Ref. 18, and β is the ratio of the velocity of the incident electron to the velocity of light. Here $J_{\rm eff}(q,K)$ is defined operationally as the effective electron scattering Compton profile.

Since the continuum generalized oscillator strength can be related to the second-order differential cross section as

$$\frac{df(E,K)}{dE} = \frac{Ek(K^2 - E^2/4c^2)^2(1-\beta^2)}{4[1 - E(1-\beta^2)^{1/2}/2c^2]\,k(E)K^2F_{ex}^R}\left(\frac{d^2\sigma}{dE\,d\Omega}\right), \tag{2}$$

the effective electron Compton profile defined in Eq. (1) can be related directly to the GOS as

$$J_{\rm eff}(q,K) = \frac{2K^3}{E}\,\frac{df(K,E)}{dE} = 2K\sum_n \left|\langle \Psi_n | \sum_{i=1}^{N} e^{i\vec{K}\cdot\vec{r}_i} | \Psi_0 \rangle\right|^2 \delta(E_n - E), \tag{3}$$

where, in this case, Ψ_n is the wave function for the final ion state, including the ejected electron, and q is related nonrelativistically to the energy loss and the momentum transfer by

$$q = (E - K^2)/2K. \tag{4}$$

While Eq. (3) is a valid definition of an effective Compton profile as long as the first Born theory is valid and exchange corrections are small, it will be of theoretical interest only if $J_{\rm eff}(q,K)$ is independent of K over an extended range of K. That is, we are interested in finding out if an experimental $J_{\rm eff}(q,K)$ has more than one plateau region in a plot of $J_{\rm eff}(q_0,K)$ vs K with q_0 a fixed constant value of q. That is, any time a binary encounter mechanism is applicable $J_{\rm eff}(q,K)$ will depend only on q. Note that $J_{\rm eff}(q_0,K)$ always has at least one plateau region which is the binary encounter limit as $K \to \infty$, and leads to the usual total x-ray Compton profile. If additional plateau regions are defined experimentally, a question arises as to whether these are due to the binary encounter approximation being fulfilled for the target electrons included in the spectrum at the energy loss under consideration, or are these only intermediate situations which can only be predicted by use of Eq. (3) with explicit use of final ion eigenstates? It is worth noting in this connection the recent exact hydrogenic (EH) type calculations of Eisenberger and Platzman,[19] and Mendelsohn and Bloch,[14] which make explicit use of approximations to the final ion eigenstates. These results can be contrasted with the impulse type (IA) calculations,[19] which use ground-state momentum densities for the electrons in the shell or shells in question.

For atoms and molecules with more than one shell and with shell binding energies separated by several hundred electron volts (e.g., the ionization potentials for the $2p$ and $2s$ electrons of Ar are 245 and 320 eV, respectively, 410 eV for the N_2 $1s$ electrons, and 870 eV for the Ne $1s$ electrons), it is possible to choose a scattering angle such that the peak position of the Bethe ridge, given approximately by $E = K^2 - E^2/4c^2$, and an appreciable section of the generalized oscillator strength on the high-energy loss side will lie below (smaller q) the first energy loss corresponding to the excitation and ionization of electrons in the next inner shell. This part of the generalized oscillator strength, assuming no important interactions with electrons in the next inner shell, will lead to a Compton profile as defined by Eq. (3), which we will here call an experimental cumulative Compton profile. The cumulative Compton profile defined in this way, though often limited in its q range by the energy loss corresponding to the excitation of the next inner-shell electrons, can be expected to

contain new and interesting information concerning electrons in its shell(s). The word cumulative is used since we might expect to see three plateau regions in a system such as Ar, with the first (smallest K) plateau corresponding to contributions from the M shell, the second to the sum of contributions from the M and L shells, and the third and last to the total of the sum of all three shells.

III. EXPERIMENTAL

The high-energy electron-impact spectrometer used in this study has been described extensively elsewhere.[17] The apparatus, employing a Möllenstedt energy analyzer[20] and a silicon surface-barrier detector, was operated with a variable energy resolution between 3–7 eV full width at half-maximum (FWHM), so that the experimental broadening of the natural line shape of the Compton profile could be made negligible. An incident electron beam of 20–400 μA accelerated to 25 keV with a telefocus electron gun[21] was directed to impinge at right angles on a gas jet eminating from a Pt nozzle of 0.15 mm i.d. and 6 mm throat length. The electron beam size was about 300–500 μm FWHM. The position of the nozzle was carefully adjusted to eliminate nozzle scattering. A typical gas flow rate was about 10^{19} atom (molecule)/sec, which produced a local target density of 10^{-1}–10^{-2} Torr in a 1 mm^3 scattering volume. The background pressure during the experiment was never allowed to exceed 3.5×10^{-5} Torr. Energy-loss spectra were taken over a range of 2 eV–2.5 keV in a signal averaging mode, using a 512 channel Northern Scientific NS 600 Multichannel analyzer. The analyzer resolution was normally about 5 V/channel and the dwell time per channel was 0.9 sec. A typical scan took 8 min, and the measurement at a particular angle required from 25 min for a 3° scattering angle to slightly less than 4 h for a 12° scattering angle. Measurements were made at two different pressures to test for the presence of multiple scattering. A more detailed discussion of the effects of multiple scattering is included in Sec. IV. In the case of N_2 observations were made at 35 and 45 keV to test for possible failure of the first Born approximation. These tests showed no differences in the GOS's at the 1% accuracy level when plotted as a function of K. The angles at which the valence profiles were obtained were 4°–5° for N_2, 8°–9.5° for Ne, 3°–4° for the M shell of Ar, and 9°–12° for the L-plus-M shell of Ar. For the total Compton profile of N_2 data were taken in the region 9°–12°.

IV. DATA ANALYSIS

The relative differential cross section measured at each scattering angle, after being converted to a generalized oscillator strength according to Eq. (2), was normalized to an absolute scale by use of the Bethe sum rule[16]

$$S(0,K)=\int_0^\infty \frac{df(E,K)}{dE}\,dE=N, \tag{5}$$

where N is the total number of electrons in the target system. In the case of Ar the K-shell electron binding energy is at 3.2 keV, which would necessitate collecting data up to at least 6–7 keV for proper normalization. Because the GOS goes nearly to zero before the energy loss reaches 3.2 keV, we have normalized the GOS in Ar by stopping the sum before 3.2 keV and matching the area to 16 instead of 18 electrons.[22] Suitable corrections were also applied for the missing area to the L-plus-M shells. Unlike the experiments for He and H_2, where the GOS measured at 7°–10°, vanished beyond an energy loss of about 1400 eV, the GOS due to the ionization of the inner-shell electrons will usually extend beyond the present maximum measured energy loss of 2.5 keV. The extent depends on the number and the binding energies of the inner-shell electrons. In this study, the percentage of the area under the GOS beyond the maximum measured energy loss is largest in Ar and smallest in N_2. The asymptotic behavior of the generalized oscillator strengths with respect to the energy loss at large energy loss has been shown for atoms to be[23]

$$\frac{df(E,K)}{dE}\propto E^{-(3.5+l)}, \tag{6}$$

where l is the angular momentum quantum number of the electron in the initial state. However, the situation is further complicated by the existence of a constant experimental background[6,24] due to detector noise and the scattering of stray electrons from chamber walls and slits. An energy-loss spectrum taken under the same condition at a much smaller angle where the GOS is known to vanish at a smaller energy loss can provide an estimate of the upper limit of the background contribution. The constant background was then determined by a least-squares fitting of the tail of the energy-loss spectrum by using Eq. (6) and Eq. (2) to determine $d^2\sigma/d\Omega\,dE$ with an added constant term to simulate the background. The background thus obtained was usually found to be quite consistent with known experimental conditions such as the number of scans, the incident electron current, and the target gas flow rate. Note also that the background is usually less than 20 counts/channel as compared to more than 10 000 counts/channel at the top of the Compton profile; therefore, the uncertainty in the background is small, especially when compared to that reported in x-ray Compton

experiments. This background was then subtracted from the signal, and the area missing from the integral in Eq. (5), due to the finite energy-loss range, was estimated. In all cases, the estimated missing area was below 7.2% of the total area, ranging from 0.3% for N_2 at 4° to 7.2% for Ar at 12°.

The correction owing to the fact that the energy-loss spectrum was taken at constant angle instead of constant momentum transfer, as required in the Bethe sum-rule normalization,[25] was also considered. Although the energy-loss spectrum for these target systems with core electrons are much broader than those for He and H_2, the choice of scattering angle for normalization purposes could always be taken large enough so that the correction due to a nonconstant value of K was estimated to be less than 1%.

An independent check of the normalization can be made in the case of the total Compton profile of N_2 and the L-plus-M-shell Compton profile of Ar by integrating the Compton profile on the positive q side, where the normalization condition

$$\int_0^\infty J_{\text{eff}}(q,\infty)\,dq = \tfrac{1}{2}N, \tag{7}$$

with N the number of electrons in the shell(s) under consideration, would be satisfied if the binary encounter theory were valid. This procedure, while giving almost complete agreement for He for scattering angles larger than 8° and for H_2 for scattering angles larger than 5°, showed a slight discrepancy between theory and experiment, of less than 2%, for the integral in Eq. (7). Possible reasons for this discrepancy, other than a failure of the binary encounter theory, are interatomic (intermolecular) multiple scattering and nozzle scattering. All of these reasons will make $J_{\text{eff}}(q)$ higher on the negative q side. Note that this test could not be carried out for the other valence profiles studied here, because the position of the excitation and ionization spectrum of the core electrons did not allow the extraction of a sufficient q range.

Interatomic (intermolecular) multiple scattering is more serious in heavy systems than in light ones. According to the proposed mechanism, which has been confirmed by several electron-impact experiments,[26] the most likely cause of multiple scattering is for an electron to be scattered inelastically at, or near, zero angle from one scatterer and then undergo a second elastic scattering from another scatterer at, or near, the scattering angle at which the measurement is made. The reverse process should be equally probable, and the resulting contribution to the scattering similar in nature. Because of the rapidly increasing dominance of the elastic scattering (which increases with atomic number roughly as Z^2) as the atomic number increases, multiple scattering is expected to affect the inelastic scattering cross section (which increases with atomic number as Z) more seriously for the heavier elements. The flow rate of the gas through the jet in these experiments was carefully controlled and kept as low as possible while still producing a reasonable counting rate for the scattered electrons. Because the multiple scattering will contribute more to the low energy-loss region of the spectrum, the sum[16]

$$S(-1,K) = \int_0^\infty E^{-1}\frac{df(E,K)}{dE}\,dE, \tag{8}$$

which relates to the x-ray incoherent scattering factor $S(K)$ according to

$$S(K) = K^2 S(-1,K), \tag{9}$$

and is more sensitive to the low energy-loss part of the spectrum, can sometimes be used as a test for whether or not significant multiple scattering effects exist. Theoretical values for $S(K)$ are often available for comparison.[27] A consistently higher experimental $S(K)$ would suggest significant multiple scattering contributions to the energy-loss spectrum. An inspection of the $S(K)^{\text{expt}}$ in this study showed only random departures from the best available theoretical values. Although this diagnosis is by no means absolute, it is nevertheless possible to estimate that the multiple scattering effects on the Compton profiles in the present experiments should be less than 1%.

In spite of the fact that the scattering angle was carefully calibrated with a high precision potentiometer, it was necessary to include a slight readjustment of the value for the angle in the data analysis by fitting the Compton profile near $q = 0$ (usually from $q = -0.5$ to $+0.5$ a.u.) with a polynomial of the form $a + bq^2 + cq^4$. The angle was adjusted until the Compton profile became symmetrical within this q range. The uncertainty in determining the center of the profile is estimated to be within ±0.02 a.u. in q, although the determination of the actual scattering angle may be as large as ±0.1° in the worst case. This angular discrepancy is thought to arise from the motion of the electron gun through slight variations, ±60 mG, in the magnetic field of the scattering chamber. These small field changes are thought to cause slight alterations in the direction of the electron beam incident upon the gas jet.

This fitting of $J(q)$ for small q also yields estimates of certain properties of the one electron momentum density. Let the Compton profile be represented in the following form:

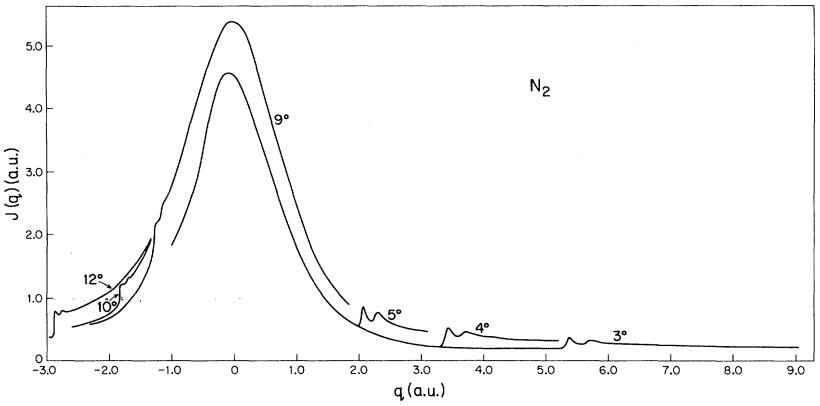

FIG. 2. Effective Compton profiles for N_2 determined by use of 25-keV incident energy electrons at scattering angles of 4°, 5°, 8°, 9°, 10°, and 12°. Data are plotted on an absolute scale determined by use of the Bethe sum rule. Note that differences between the 4° and 5° data and the 8°—12° data are indistinguishable in the region near $q=0$ on the plotted scale.

$$J(q)=2\pi\left(\int_0^\infty dp\, p\rho(p)-\int_0^q dp\, p\rho(p)\right), \tag{10}$$

and expand $\rho(p)$ in a Taylor series as

$$\rho(p)=\rho(0)+\tfrac{1}{2}p^2\rho''(0)+\cdots, \tag{11}$$

since $\rho(p)$ is an extremum at $p=0$. Hence it is obvious that in the region of small q, the Compton profile can be expanded in terms of q^2 as[28]

$$J(q)=\tfrac{1}{2}\{\langle p^{-1}\rangle-\tfrac{1}{2}q^2[4\pi\rho(0)]-\tfrac{1}{8}q^2[4\pi\rho''(0)]+\cdots\}, \tag{12}$$

where $\langle 1/p\rangle$, $\rho(0)$, and $\rho''(0)$ can then be determined from least-squares fitting of experimental data.

In addition to the treatment of the small-angle data, a function of the form

$$J(q)=\sum_{n=1}^{M}\frac{a_n}{[1+q^2/\xi(n)^2]^{2n+1}} \tag{13}$$

for the Compton profile with $\xi(n)=\xi_0/n$, was found to provide an excellent fit of the experimental data over the complete data range. To avoid convergence problems with the use of nonlinear parameters the coefficients a_n were determined for fixed ξ_0 by linear least squares. The procedure was repeated over a grid of ξ_0 values until the minimum was found. The functional dependence given by Eq. (13) leads to simple analytical forms for the momentum density and all its important properties. These are

$$\rho(q)=\frac{1}{\pi}\sum_{n=1}^{M}\frac{(2n+1)a_n\,\xi(n)^{4n+2}}{[\xi(n)^2+q^2]^{2n+2}}, \tag{14a}$$

$$\rho(0)=\frac{1}{\pi}\sum_{n=1}^{M}\frac{(2n+1)a_n}{\xi^2(n)}, \tag{14b}$$

$$\rho''(0)=-\frac{4}{\pi}\sum_{n=1}^{M}\frac{(n+1)(2n+1)a_n}{\xi(n)^4}, \tag{14c}$$

$$\langle q^{2l}\rangle=\pi\sum_{n=1}^{M}a_n\,\xi(n)^{2l+1}\,\frac{(2l+1)!!\,(4n-2l-1)!!}{(4n)!!}$$

$$[-1\leq l\leq 2;\ (-1)!!=1], \tag{14d}$$

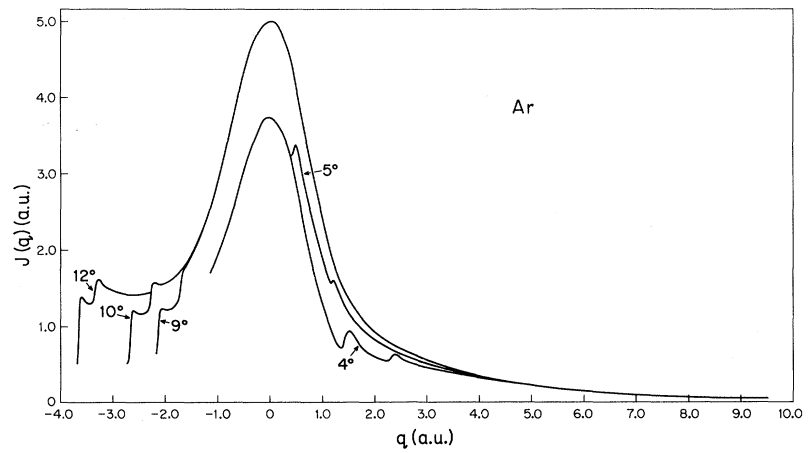

FIG. 3. Effective Compton profiles for Ar determined by use of 25-keV incident energy electrons at scattering angles of 4°, 5°, 9°, 10°, and 12°. Data are plotted on an absolute scale determined by use of the Bethe sum rule for assuming only 16 electrons in the atom. Note that differences between the 4° and 5° data and the 9°—12° data are indistinguishable in the region near $q=0$ on the plotted scale.

and

$$\langle q^{2l+1}\rangle = 2\sum_{n=1}^{M} a_n\, \xi(n)^{2l+2}\, \frac{(l+1)!\,(2n-l-1)!}{(2n)!} \qquad (-1 \leq l \leq 1), \quad (14e)$$

where all these results can be readily derived from Eq. (13) and the well-known relation

$$\rho(q) = -\frac{1}{2\pi q}\,\frac{dJ(q)}{dq}\,.$$

V. RESULTS AND DISCUSSION

The most striking qualitative proof of the existence of valence or cumulative shell Compton profiles is given in Figs. 2 and 3. Note how well the effective Compton profiles superimpose in each momentum transfer region, and how each point takes a "quantum jump" upwards as the spectral region of the next innermost shell passes by, moving toward smaller q values. Once this "quantum jump" wave has passed through the profile, note how the newly assumed shape is again nearly independent of K. For a more detailed analysis of this behavior the reader is referred to the actual experimental values of the valence Compton profile and the total Compton profile of N_2, the L-shell Compton profile of Ne, the M shell and the M-plus-L shell Compton profiles of Ar, which are given in Tables I–V. They are compared with other experimental (x-ray, γ-ray) Compton profiles and various theoretical calculations where available. Certain momentum space properties such as $\langle 1/p\rangle$, $\rho(0)$, and $\rho''(0)$ deduced from the experimental data by use of Eq. (12) are also presented in these tables. In Table VI the parameters for the least-squares fit of the profile data at certain angles are given. Finally the results obtained from these parameters for the properties listed in Eqs. (14b)–(14e) are given in Table VII.

It needs to be pointed out that in some cases several minima in the standard deviation for the least-squares fits as a function of ξ_0 were observed. Some fits with multiple minima even had similar standard deviations for the same number of terms. We have selected the solution set with the smallest standard deviation. In the cases of greatest ambiguity the other solutions lead to values for the moments well within our assigned uncertainties. The reported fits contain the largest number of parameters for which the total standard deviation still made a significant change in comparison to the fit with one less parameter. The uncertainties in the a_n's are those predicted by the least-squares analysis, while a 10% uncertainty was assigned to ξ_0 on the basis of the observed variation in the total standard deviation as a function of variations in ξ_0. The values for $\rho(0)$, $\rho''(0)$, and $\langle 1/p\rangle$ all appear to be in good agreement with those obtained from the use of Eq. (12). In addition the estimates for $\langle p^0\rangle$ appear to be in reasonable agreement with expectation, and the value of $\langle p^2\rangle$ for the total N_2 profile which should have the same magnitude as the total electronic energy of N_2 appears to be reasonable. Clearly the higher moments, which depend more strongly on data at large q values which have larger associated uncertainties, will be least reliable. A good many of the moments reported in Table VII are given here for the first time, and it will be interesting to see how they will compare with future theoretical calculations.

The usual x-ray Compton profile given as

$$J(q) = 2\pi \int_q^\infty \rho(p)\, p\, dp \qquad (15)$$

must, of course, be independent of the momentum

TABLE I. Effective valence-shell Compton profile of N_2 obtained with 25-keV incident energy electrons.

	This work		
q	4° (K^2 = 9.39 a.u.)	5° (K^2 = 14.5 a.u.)	Theory [a]
0	4.891	4.968	4.794
0.1	4.849	4.871	4.748
0.2	4.606	4.802	4.618
0.3	4.378	4.475	4.414
0.4	4.117	4.109	4.141
0.5	3.725	3.851	3.821
0.6	3.359	3.475	3.471
0.7	2.927	3.033	3.106
0.8	2.572	2.704	2.742
0.9	2.269	2.354	2.391
1.0	1.966	2.024	2.065
1.2	1.390	1.484	1.501
1.4	1.026	1.039	1.068
1.6	0.730	0.760	0.751
1.8	0.594	0.558	0.522
2.0	0.417		0.373
2.2	0.324		
2.4	0.238		
2.6	0.179		
2.8	0.145		
3.0	0.107		
$\rho(0)$	1.82 ± 0.14	1.75 ± 0.13	
$\rho''(0)$	−7.0 ± 3.0	−5.6 ± 2.4	

[a] S. R. Langhoff (private communication). These values are based on nonrelativistic restricted Hartree-Fock (RHF) calculations with electron correlation corrections obtained from Gaussian orbital configuration interaction (CI) calculations, added on. The CMO NK-shell Compton profile has been subtracted from this total result to obtain the valence-shell result.

TABLE II. Total Compton profile of N_2 obtained with 25-keV incident energy electrons.

	This work			
q	8° (K^2=37.3 a.u.)	9° (K^2=46.7 a.u.)	10° (K^2=58.9 a.u.)	12° (K^2=84.9 a.u.)
0	5.343	5.392	5.414	5.399
0.1	5.339	5.360	5.204	5.229
0.2	5.121	5.123	5.173	5.217
0.3	4.877	4.963	4.948	4.906
0.4	4.564	4.591	4.601	4.667
0.5	4.251	4.294	4.236	4.189
0.6	3.801	3.786	3.915	3.916
0.7	3.446	3.562	3.537	3.460
0.8	3.101	3.110	3.157	3.186
0.9	2.649	2.747	2.722	2.785
1.0	2.356	2.375	2.409	2.374
1.2	1.782	1.828	1.880	1.858
1.4	1.373	1.422	1.439	1.408
1.6	1.116	1.158	1.092	1.119
1.8	0.874	0.922	0.880	0.861
2.0	0.691	0.722	0.682	0.720
2.5	0.471	0.454	0.468	0.475
3.0	0.349	0.362	0.336	0.363
3.5	0.260	0.274	0.265	0.249
4.0	0.203	0.197	0.207	0.173
4.5	0.165	0.153	0.144	0.154
5.0	0.130	0.137	0.132	0.109
$\rho(0)$	1.60±0.14	1.42±0.17	1.46±0.14	1.66±0.19
$\rho''(0)$	−1.9±2.5	1.1±3.9	−1.2±2.3	−8.2±5.2

			Theoretical calculations [c]	
q	x-ray [a]	γ-ray [b]	CI	RHF
0	5.327	5.325	5.315	5.343
0.1	5.277	5.282	5.269	5.299
0.2	5.142	5.153	5.138	5.169
0.3	4.924	4.947	4.932	4.964
0.4	4.631	4.676	4.656	4.689
0.5	4.286	4.354	4.333	4.364
0.6	3.914	4.000	3.974	4.006
0.7	3.523	3.630	3.609	3.629
0.8	3.153	3.259	3.239	3.251
0.9	2.803	2.901	2.882	2.887
1.0	2.476	2.568	2.549	2.546
1.2	1.934	1.997	1.971	1.958
1.4	1.527	1.559	1.521	1.503
1.6	1.230	1.234	1.185	1.168
1.8	0.997	0.991	0.937	0.922
2.0	0.821	0.805	0.764	0.751
2.5	0.542	0.521	0.510	0.504
3.0	0.390	0.396	0.381	0.378
3.5	0.310	0.295	0.296	0.295
4.0	0.244	0.234	0.235	0.234
4.5				
5.0		0.143	0.148	0.148
		$\rho(0)$ [c]	1.23	1.20
		$\rho''(0)$ [c]	−1.80	1.00

[a] Reference 28.
[b] Reference 29.
[c] S. R. Langhoff (private communication). See footnote a of Table I for further details.

transfer. This condition will be satisfied if the binary encounter approximation (impulse approximation) is fulfilled. However, it may be possible to still have a dependence on the final ion eigenstate with an effective profile depending only on q.[15] The only requirement is that the Compton profile will have to be independent of the momentum transfer over a finite region of K values. Such behavior has been observed in He and H_2, but this most certainly is associated with an approach to the expression given in Eq. (15). Here we obviously have several experimentally defined plateau regions well before the binary encounter theory can be expected to be valid for the total systems. The question is: does a limited form of the binary encounter theory hold for subshells in a certain range?

In N_2, true plateau regions appear to have been reached in this study for both the valence Compton profile at 4°–5°, and the total Compton profile at 8°–12° at the 2% level for q values near the peak maximum. It is obvious from Tables I and II that $J(q)$ is independent of momentum transfer in these regions, with the differences between the various Compton profiles taken within these regions being entirely within the statistical uncertainty. Comparing with the experimental results from x-ray[28] and γ-ray Compton scattering[5b,29] and theoretical calculations,[30] it is apparent that the total Compton profile reported in this study is slightly higher and sharper than previous results, but by an amount small or comparable to experimental uncertainty. However, the valence Compton profile is more than 2% higher at the Compton peak as the result of a narrower profile

TABLE III. Ar M-shell effective Compton profile obtained with 25-keV incident energy electrons.

q	4° (K^2 = 9.39 a.u.)	5° (K^2 = 14.5 a.u.)
0	3.826	3.846
0.1	3.821	3.847
0.2	3.713	3.731
0.3	3.541	3.585
0.4	3.262	
0.5	2.932	
0.6	2.628	
0.7	2.266	
0.8	1.944	
0.9	1.651	
1.0	1.392	
1.2	0.958	
ρ (0)	1.03 ± 0.09	1.20 ± 0.13
ρ'' (0)	2.3 ± 2.0	−4.1 ± 3.4

TABLE IV. Ar L + M-shell effective Compton profile obtained with 25-keV incident energy electrons.

	This work			Theoretical[b] (RHF) (total	γ-ray[a] (total profile)
q	9° (K^2 = 46.7 a.u.)	10° (K^2 = 58.9 a.u.)	12° (K^2 = 84.9 a.u.)	profile)	
0	4.934	4.990	4.946	5.05	5.118
0.1	4.895	4.968	4.986	5.03	5.082
0.2	4.752	4.831	4.806	4.95	4.976
0.3	4.676	4.624	4.602		4.806
0.4	4.327	4.388	4.440	4.61	4.581
0.5	4.032	4.099	4.077		4.310
0.6	3.703	3.746	3.655	4.03	4.007
0.7	3.311	3.436	3.353		3.686
0.8	3.049	3.007	2.953		3.357
0.9	2.650	2.684	2.611		3.034
1.0	2.364	2.413	2.351	2.66	2.726
1.2	1.852	1.905	1.800		2.184
1.4	1.484	1.504	1.476		1.765
1.6	1.253	1.297	1.225		1.467
1.8	1.069	1.089	1.057		1.266
2.0	0.947	0.934	0.921	1.08	1.128
2.5	0.730	0.727	0.672		0.899
3.0	0.551	0.562	0.522		0.737
3.5	0.472	0.441	0.430		0.626
4.0	0.357	0.343	0.349	0.521	0.525
4.5	0.285	0.261	0.263		
5.0	0.245	0.227	0.209		0.357
ρ (0)	1.12 ± 0.11	1.29 ± 0.11	1.47 ± 0.13		
ρ'' (0)	1.82 ± 2.2	−3.0 ± 2.2	−12.0 ± 6.0		

[a]Reference 29.

[b]Reference 30.

TABLE V. Ne L-shell effective Compton profile obtained with 25-keV incident energy electrons.

q	7° (K^2=30.2 a.u.)	8° (K^2=37.6 a.u.)	x-ray [a]	EH [b]	Impulse (HF) [b]
0	2.734	2.677	2.598	2.609	2.548
0.1	2.751	2.681	2.592	2.612	2.540
0.2	2.712	2.643	2.577	2.595	2.516
0.3	2.653	2.560	2.533	2.557	2.475
0.4	2.578	2.509	2.465	2.498	2.415
0.5	2.475	2.385	2.369	2.419	2.335
0.6	2.356	2.334	2.255	2.300	2.237
0.7	2.251	2.143	2.126	2.206	2.120
0.8	2.024	1.983	1.984	2.078	1.993
0.9	1.903	1.804	1.836	1.940	1.856
1.0	1.755	1.709	1.679	1.796	1.715
1.2	1.410	1.401	1.390	1.505	1.436
1.4	1.178	1.106	1.145	1.228	1.178
1.6	0.944	0.898	0.930	0.982	0.953
1.8	0.769	0.723	0.754	0.774	0.766
2.0	0.602	0.573	0.605	0.605	0.614
2.5	0.346		0.347	0.328	0.355
$\rho(0)$	0.54±0.13	0.53±0.13			
$\rho''(0)$	−4.3±2.5	−3.3±2.5			

[a] Reference 28.

[b] Reference 14b.

than that obtained from x-ray and γ-ray studies by subtraction of theoretical estimates for the core contribution. It is worth pointing out here that almost all known experimental errors, such as multiple scattering, nozzle scattering, the effect of finite energy resolution (which is extremely small in this study), and all known background contributions, tend to make the Compton profile broader and as a consequence usually lower. Therefore it is unlikely that the observed discrepancy is due to experimental errors. There are, however, two possible explanations for this discrepancy. Smith and Whangbo,[11] in their theoretical study of localized molecular orbitals (LMO), suggested that because the LMO electron distribution is much more contracted than the canonical molecular orbitals (CMO) for the core electrons, that the LMO momentum space core should have a larger contribution from the high momentum region. These authors showed by their calculation that the LMO core Compton profile is broader and lower than that for the CMO core. The difference, according to their calculation, is about 1.2% of the valence profile at $q=0$. It must be kept in mind, however, that this mechanism is restricted to the molecular case. The "experimental" valence Compton profiles in the x-ray and γ-ray experiments were deduced from the total Compton profile by subtracting out the CMO core Compton profile. This makes the valence profile appear lower and broader than that obtained if the LMO core profile were subtracted out. The second factor is in the experimental definition of the effective Compton profile. It was pointed out in Sec.

TABLE VI. Parameters obtained from least-squares fits of the Compton profiles by the expression

$$J(q)=\sum_{n=1}^{3}\frac{a_n}{[1+q^2/\xi^2(n)]^{2n+1}} \quad \text{with } \xi(n)=\xi_0/n .$$

	N_2		Ne		Ar		
	4°	12°	7°	8°	4°	10°	12°
ξ_0	6.73±0.67	7.42±0.74	5.62±0.56	5.19±0.53	3.43±0.34	7.15±0.72	7.07±0.07
a_1	$(4.5\pm9.6)\times10^{-2}$	0.37±0.10	0.35±0.08	0.66±0.10	0.63±0.10	0.78±0.09	0.77±0.12
a_2	1.44±0.27	1.03±0.30	2.68±0.24	2.17±0.28	3.86±0.27	0.89±0.30	0.83±0.39
a_3	3.36±0.22	3.94±0.27	−0.29±0.21	−0.13±0.21	−0.62±0.20	3.39±0.28	3.45±0.35

II that the Compton profile defined in an electron scattering experiment according to Eq. (3) involves explicit summation over all possible transitions to final ion states. Strictly speaking, this is also true in the photon scattering case.[14] This resembles more closely the exact hydrogenic (EH) calculation of Bloch and Mendelsohn.[14] Their calculations on other systems, such as Ne, Ar, and Si, usually give higher and sharper profiles than those based on impulse type calculations. The difference ranges from 2.4% for Ne to 5.6% for Ar.

An "experimental" core profile was obtained for N_2 from the difference between the observed total and valence Compton profiles. It appears to agree better with the LMO calculation. However, it must be kept in mind that it was obtained from the difference of two much larger quantities, and the dependence on the final ion eigenstates as a possible cause has been ignored. The realistic uncertainties in the total profile and the valence profile are on the order of (1–2)% near the maximum. This leads to a (15–30)% uncertainty in the estimation of the core Compton profile. Therefore, we cannot definitely conclude that the LMO core profile is closer to the "true" experimental core profile.

The Compton profiles for the Ar M shell at 4° and 5°, and the Ar M-plus-L shell at 9°, 10°, and 12° showed, in contrast to N_2, a small but definite trend with scattering angle. In a given plateau region the $J_{\text{eff}}(q,K)$ obtained at a larger momentum transfer is higher and sharper than those obtained at smaller K values. This trend is in the direction predicted by the binary encounter approximation. Preliminary data were also taken at scattering angles smaller than the above mentioned angular range but the results showed that the value of an effective $J_{\text{eff}}(q,K)$ was extremely sensitive to variations in K. An estimate of the total Compton profile was not obtained in this study owing to the present limitations on our angular range. However, we can estimate a total $J(q)$ from our results by adding a theoretical K-shell contribution, which gives us values very close to the γ-ray result of Eisenberger and Reed,[5b,31] and slightly higher than most of the theoretical calculations based on the impulse approximation.[29] It would, therfore, be closer to the EH calculations of Bloch and Mendelsohn.[14] No M-shell Compton profile for Ar has yet been reported in the literature, however an estimate of the L-shell Compton profile for Ar from this experiment was obtained from the difference of the M-plus-L-shell profile and the M-shell profile. The $J(0)$ value from this experimental difference profile is 1.100, which is in very good agreement with the value of 1.077 given by the EH method as reported in Ref. 14b.

The results for Ne behaved in a similar way to those for Ar. The data up to 8° showed a definite

TABLE VII. Some properties of the momentum distributions for N_2, Ne, and Ar in Rydberg atomic units.

	N_2		Ne	
	4° (valence)	12° (total)	7° (L shell)	8° (L shell)
$\rho(0)$	1.7 ± 0.4	1.56 ± 0.31	0.35 ± 0.19	0.43 ± 0.21
$\rho''(0)$	−5 ± 2	−4 ± 2	0.06 ± 0.8	−0.36 ± 0.10
$\langle p^{-2}\rangle$	17.2 ± 1.8	17.1 ± 1.9	6.3 ± 1.5	6.5 ± 1.6
$\langle p^{-1}\rangle$	9.70 ± 0.72	10.7 ± 0.8	5.47 ± 0.69	5.39 ± 0.73
$\langle p^{0}\rangle$	9.87 ± 1.33	13.4 ± 1.6	8.44 ± 1.12	8.73 ± 1.15
$\langle p^{1}\rangle$	15.8 ± 5.0	36 ± 7	21.5 ± 4.2	25.1 ± 4.4
$\langle p^{2}\rangle$	44 ± 36	210 ± 71 [a]	96 ± 30	123 ± 31
$\langle p^{3}\rangle$	$(2.6 \pm 4) \times 10^2$	$(2.3 \pm 1.1) \times 10^3$	$(7.7 \pm 3.3) \times 10^2$	$(9.9 \pm 3.4) \times 10^2$
$\langle p^{4}\rangle$	$(4 \pm 8) \times 10^3$	$(5.0 \pm 2.8) \times 10^4$	$(1.2 \pm 0.7) \times 10^4$	$(1.5 \pm 0.6) \times 10^4$

	Ar		
	4° (M shell)	10° ($M+L$ shell)	12° ($M+L$ shell)
$\rho(0)$	1.08 ± 0.63	1.44 ± 0.28	1.50 ± 0.32
$\rho''(0)$	4 ± 1	−4 ± 1	−4 ± 2
$\langle p^{-2}\rangle$	13.5 ± 2.8	15.5 ± 1.8	15.9 ± 2.1
$\langle p^{-1}\rangle$	7.73 ± 0.70	10.0 ± 0.8	10.1 ± 1.1
$\langle p^{0}\rangle$	7.72 ± 0.84	14.9 ± 1.6	14.7 ± 1.9
$\langle p^{1}\rangle$	12.8 ± 2.1	52 ± 10	50 ± 10
$\langle p^{2}\rangle$	37 ± 10	359 ± 112	345 ± 109
$\langle p^{3}\rangle$	$(1.9 \pm 0.7) \times 10^2$	$(4.1 \pm 1.8) \times 10^3$	$(3.9 \pm 1.7) \times 10^3$
$\langle p^{4}\rangle$	$(1.8 \pm 0.8) \times 10^3$	$(8.6 \pm 4.7) \times 10^4$	$(8.1 \pm 4.2) \times 10^4$

[a] The RHF value is 217.76 Ry. S. R. Langhoff (private communication).

trend of changing to a sharper and higher profile as the scattering angle increased. It is apparent that 8° is not yet in the region where $J(q)$ is independent of angle. Another measurement at 9° at a later time showed a slightly lower and broader profile, but the difference was well within experimental uncertainties. However, both the 8° and 9° profiles are several percent higher than the x-ray Compton profile and the impulse calculations. It has been shown by several theoretical studies[32] that wave functions for Ne with or without electron correlation give practically the same Compton profile. Therefore, the most likely cause for the disagreement is again the difference in the experimental definition of our effective Compton profile. This conclusion is supported by EH results given in Ref. 14b, although our profile is nearly 2% higher at the maximum than these calculations.

We conclude from the foregoing observations made on N_2, Ne, and Ar that the observed sharpening of valence-shell Compton peaks must be due to an explicit dependence on the final ion eigenstate rather than a difference in the definition of localization of molecular orbitals. It is still possible however to interpret the profile in terms of ground state properties, as we have done in Table III, providing conclusions drawn from such a comparison properly reflect the error inherent in the use of a different operational definition for the Compton profile. For the profiles reported in this study the differences in $J(0)$ due to different definitions is probably within 5% at the profile maximum. Other properties can of course be effected in a more sensitive way.

It is interesting to observe that the value of $\rho(0)$ does not change appreciably when a new (inner) shell of electrons is included into the measurement. If hydrogenic wave functions are used for an order-of-magnitude calculation, it can be shown that p electrons do not contribute to $\rho(0)$, and the s electron contributions are

$$\rho(0)_{1s} = (8/\pi^2)\,1/Z_{1s}^3 \text{ per electron},$$

$$\rho(0)_{2s} = (256/\pi^2)\,1/Z_{2s}^3 \text{ per electron},$$

$$\rho(0)_{3s} = (2904/\pi^2)\,1/Z_{3s}^3 \text{ per electron}.$$

Using Slater's values for the orbital exponent, it is obvious that each successive inner-shell electron contribution will be at least an order of magnitude smaller than the previous value.

The results for $\rho(0)$ listed in Tables I–V show semiquantitative agreement with this simplified calculation. It has been proposed[30] that $\rho(0)$ and especially $\rho''(0)$ should be very sensitive to the details of the electron correlation in the wave functions used. The values of $\rho(0)$ obtained in our experiment are quite consistent and should provide a good test for theoretical calculations within the 10% experimental uncertainty. The uncertainty of $\rho''(0)$ is rather large, making an estimate of its exact value difficult, but these values may still prove useful for establishing the correct order of magnitude and sign. The sign of the average value of $\rho''(0)$ was generally negative with the exception of the Ne L shell in the observations reported here. Langhoff[30] has predicted a value for $\rho''(0)$ in the case of N_2, using an SCF wave function of 1.0, while with a configuration interaction (CI) wave function he found a value of −1.8. It appears that although only very rough estimates of $\rho''(0)$ can be obtained from experiment, they may still prove to be useful because of the apparent extreme sensitivity to electron correlation effects.

In previous experimental studies of Compton profiles, the authors have mainly reported the statistical uncertainties as determined by their count rates. We believe that the systematic error in our own experiments is generally larger than this statistical uncertainty. We would suggest that workers using other measurement techniques make a careful reassessment of their own sources of systematic error. Systematic errors in our work such as the angular uncertainty, the uncertainty in the background subtraction, the effect of finite energy resolution, and errors in the normalization procedure can be as large as 2%, and are in addition to those determined from count rate statistics. We feel that at present even with $\frac{1}{2}$% or better statistical accuracy in the count rate, the accuracy in the best current electron scattering experiments are not better than 1%. We suspect similar considerations may apply to the error analysis in the x-ray and γ-ray methods.

This study demonstrates a new approach for directly measuring the Compton profile and momentum-space properties of the valence- or outer-shell electrons as well as profiles for cumulative successive shells by use of high-energy electron scattering. We have reported in this study accurate measurements for the valence and total Compton profiles of N_2. In the case of the plateau region for the Ne L-shell Compton profile and the Ar M- and M-plus-L-shell effective Compton profiles it appears that $J_{\text{eff}}(q,K)$ is still not quite independent of K. However the results found for these cases appear to be very close to available theoretical predictions and to the known result in the large momentum transfer limit. Our measurements for these three systems suggest that discrepancies exist between the impulse approximation calculations and experiment. The EH calculations which explicitly sum over all transitions to the excited ion states seem to present a better description of the experimental process. There

are still small but possibly significant discrepancies between the EH calculation and the experimental results presented here. It is, however, possible that improved calculations using more rigorous ion wave functions may reduce these discrepancies.

---

†Contribution No. 2730 from the Chemical Laboratories of Indiana University. Acknowledgment is made to the Donors of the Petroleum Research Fund, administered by the American Chemical Society, for support of this research in the form of a postdoctoral fellowship for T. C. Wong. In addition, the author gratefully acknowledges the support of the National Science Foundation Grant No. GP-41983X.

*Present address: Dept. of Chem., University of British Columbia, Vancouver, B. C., Can.

‡Permanent address: Phys. Dept., Brandeis University, Waltham, Mass. 02154

[1]A. H. Compton, Phys. Rev. 22, 412 (1923).

[2]J. W. M. DuMond, Phys. Rev. 33, 643 (1929).

[3]A. L. Hughes and M. M. Mann, Phys. Rev. 53, 50 (1938).

[4]See, for example, M. J. Cooper, Adv. Phys. 20, 453 (1971), for a review of x-ray Compton work before 1969.

[5](a) J. Felsteiner, R. Fox, and S. Kahane, Phys. Lett. 33A, 442 (1970); (b) P. Eisenberger and W. A. Reed, Phys. Rev. A 5, 2085 (1972).

[6](a) H. Schmoranzer, R. C. Ulsh, R. A. Bonham, and J. Ely, J. Chem, Phys. 59, 152 (1973); (b) H. F. Wellenstein and R. A. Bonham, Phys. Rev. A 7, 1568 (1973).

[7]I. R. Epstein, B. G. Williams, and M. J. Cooper, J. Chem. Phys. 58, 4098 (1973); R. Benesch and V. H. Smith, Jr., Chem. Phys. Lett. 5, 601 (1970); R. G. Brown and V. H. Smith, Jr., Phys. Rev. A 5, 140 (1972).

[8]C. A. Coulson, Proc. Camb. Philos. Soc. 39, 180 (1943); M. Roux and I. R. Epstein, Chem. Phys. Lett. 18, 18 (1973).

[9]I. R. Epstein, J. Chem. Phys. 53, 4425 (1970); P. Eisenberger and W. C. Marra, Phys. Rev. Lett. 27, 1413 (1971); W. A. Reed, P. Eisenberger, K. C. Pandey, and L. C. Snyder, Phys. Rev. B 10, 1507 (1974).

[10]R. C. Ulsh, R. A. Bonham, and L. S. Bartell, Chem. Phys. Lett. 13, 6 (1972).

[11]V. H. Smith, Jr., and M. H. Whangbo, Chem. Phys. 5, 234 (1974).

[12]N. C. Philips and R. J. Weiss, Phys. Rev. B 6, 4213 (1972).

[13]T. Paakkari and P. Suartti, Phys. Rev. B 9, 1756 (1974).

[14](a) B. J. Bloch and L. B. Mendelsohn, Phys. Rev. A 9, 129 (1974); (b) L. B. Mendelsohn and B. J. Bloch, Phys. Rev. A 12, 551 (1975).

[15]R. Canilloni, A. Giardini-Guidoni, R. Tribelli, and G. Steffani, Phys. Rev. Lett. 29, 618 (1972); E. Weigold, S. T. Hood, and P. J. O. Teubner, *ibid.* 30, 475 (1973); E. Weigold, S. T. Hood, I. E. McCarthy, and P. J. O. Teubner, Phys. Lett. 44A, 531 (1973); S. T. Hood, E. Weigold, I. E. McCarthy, and P. J. O. Teubner, Nat. Phys. Sci. 245, 65 (1973).

[16]M. Inokuti, Rev. Mod. Phys. 43, 297 (1971).

[17]H. F. Wellenstein, Hans Schmoranzer, R. A. Bonham, T. C. Wong, and J. S. Lee, Rev. Sci. Instrum. 46, 92 (1975).

[18] R. A. Bonham and C. Tavard, J. Chem. Phys. 59, 4691 (1973).

[19]P. Eisenberger and P. M. Platzman, Phys. Rev. A 2, 415 (1970).

[20]H. F. Wellenstein, J. Appl. Phys. 44, 3669 (1973).

[21]H. Schmoranzer, H. F. Wellenstein, and R. A. Bonham, Rev. Sci. Instrum. 46, 88 (1975).

[22]M. J. van der Wiel (private communication). The proper quantity for normalization of the $M+L$ shells is $16+\delta$, where $\delta>0$ and is given by the sum of oscillator strengths for excitation of the K-shell electrons to all higher filled orbitals. For Ne this quantity is around 0.3. We do not expect it to be terribly different here (i.e., there are more excitations possible in Ar than Ne but each contribution is much smaller in value) so that the use of 16 for normalization purposes should not introduce an error larger than about 3% in the worst case. See J. A. Bearden and J. A. Wheeler, Phys. Rev. 46, 755 (1934) for the details in the Ne case.

[23]A. R. P. Rau and U. Fano, Phys. Rev. 162, 68 (1967).

[24]Another type of background, as was pointed out in Ref. 6b, was due to the scattering of gas outside of the scattering volume. It has approximately the same shape as the signal and therefore will not affect the normalization to any significant extent.

[25]R. A. Bonham, Chem. Phys. Lett. 18, 454 (1973).

[26]T. C. Wong, J. S. Lee, H. F. Wellenstein, and R. A. Bonham (unpublished).

[27]D. T. Cramer, J. Chem, Phys. 50, 4857 (1969); C. Tavard, D. Nicolas, and M. Rouault, *ibid.* 64, 540 (1967); 64, 555 (1967).

[28]R. E. Benesch and V. H. Smith, Jr., in *Wave Mechanics, The First Fifty Years* (Wiley, New York, 1973), Chap. 21, p. 373.

[29]P. Eisenberger, Phys. Rev. A 5, 628 (1972).

[30]S. R. Langhoff (private communication).

[31]P. Eisenberger and W. A. Reed, Phys. Rev. B 9, 3237 (1974).

[32]V. H. Smith, Jr., and R. E. Brown, Chem. Phys. Lett. 20, 424 (1973).